Precision predictions for (un)stable W^+W^- pair production at and beyond CERN LEP2 energies

S. Jadach,[1,2,3] W. Płaczek,[4,3] M. Skrzypek,[2,3] B. F. L. Ward,[5,6,3] and Z. Wąs[2,3]

[1]*DESY-Zeuthen, Theory Division, D-15738 Zeuthen, Germany*
[2]*Institute of Nuclear Physics, ul. Kawiory 26a, 30-055 Cracow, Poland*
[3]*CERN, Theory Division, CH-1211 Geneva 23, Switzerland*
[4]*Institute of Computer Science, Jagellonian University, ul. Nawojki 11, 30-072 Cracow, Poland*
[5]*Department of Physics and Astronomy, The University of Tennessee, Knoxville, Tennessee 37996-1200*
[6]*SLAC, Stanford University, Stanford, California 94309*

We present precision calculations of the processes $e^+e^- \to 4$ fermions, in which the double resonant W^+W^- intermediate state occurs. Referring to this latter intermediate state as the signal process, we show that, by using the YFS Monte Carlo event generators YFSWW3-1.14 and KORALW 1.42 in an appropriate combination, we achieve a physical precision on the signal process, as isolated with CERN LEP2 MC Workshop cuts, below 0.5%. We stress the full gauge invariance of our calculations and we compare our results with those of other authors where appropriate. In particular, sample Monte Carlo data are explicitly illustrated and compared with the results of the program RACOONWW of Denner *et al.* In this way, we show that the total (physical and technical) precision tag for the *WW* signal process cross section is 0.4% for 200 GeV, for example. Results are also given for 500 GeV with an eye toward future linear colliders.

The award of the 1999 Nobel Prize for physics to G. 't Hooft and M. Veltman, and the success of the predictions of their formulation [1] of the renormalized non-Abelian quantum loop corrections for the standard model [2] of the electroweak interactions in confrontation with data of CERN e^+e^- collider LEP experiments, underscores the need to continue to test this theory at the quantum loop level in the gauge boson sector itself. This emphasizes the importance of the on-going precision studies of the processes $e^+e^- \to W^+W^- + n(\gamma) \to 4f + n(\gamma)$ at LEP2 energies [3–5], as well as the importance of the planned future higher energy studies of such processes in linear collider (LC) physics programs [6–9]. We need to stress that hadron colliders also have considerable reach into this physics and we hope to come back to their roles elsewhere [10].

In what follows, we present precision predictions for the event selections (ES) of the LEP2 Monte Carlo (MC) Workshop [11], for the processes $e^+e^- \to W^+W^- + n(\gamma) \to 4f + n(\gamma)$, based on our new exact $\mathcal{O}(\alpha)_{prod}$ Yennie-Frautschi-Suura-(YFS)-exponentiated leading-log (LL) $\mathcal{O}(\alpha^2)$ final-state radiation (FSR) leading-pole approximation (LPA) formulation, as it is realized in the MC program YFSWW3-1.14 [12,13], in combination with our all four-fermion processes MC event generator KORALW-1.42 [14,15] so that the respective four-fermion background processes are taken into account in a gauge-invariant way. Indeed, gauge invariance is a crucial aspect of our work and we stress that we maintain it throughout our calculations.

Recently, the authors in Refs. [16] have also presented MC program results for the processes $e^+e^- \to W^+W^- + n(\gamma) \to 4f + n(\gamma)$, $n = 0,1$, in combination with the complete background processes that feature the exact LPA $\mathcal{O}(\alpha)$ correction. Thus, we will compare our results, where possible, with those in Refs. [16] in an effort to check the overall precision of our work. As we argue below, the two sets of results should agree at a level below 0.5% on observables such as the total cross section.

More specifically, in YFSWW3-1.13 [13], the leading-pole approximation (LPA) is used to develop a fully gauge-invariant YFS-exponentiated calculation of the signal process $e^+e^- \to W^+W^- + n(\gamma) \to 4f + n(\gamma)$, which features the exact $\mathcal{O}(\alpha)$ electroweak correction to the production process and the $\mathcal{O}(\alpha^2)$ LL corrections to the final-state decay processes. The issue is how to combine this calculation with that of KORALW-1.42 in Refs. [14,15], for the corresponding complete Born-level cross section with YFS-exponentiated initial-state $\mathcal{O}(\alpha^3)$ LL corrections. In this connection, we point out that the LPA enjoys some freedom in its actual realization, just as does the LL approximation in the precise definition of the big logarithm L, without spoiling its gauge invariance. This can already be seen from the book of Eden *et al.* [17], wherein it is stressed that the analyticity of the S matrix applies to the scalar form factors themselves in an invariant Feynman amplitude, without any reference to the respective external wave functions and kinematical (spinor) covariants. The classic example illustrated in Ref. [17] is that of pion-nucleon scattering, with the amplitude

$$\mathcal{M} = \bar{u}(p_2)[A(s,t) + B(s,t)(\not{q}_1 + \not{q}_2)]u(p_1), \qquad (1)$$

where the p_i are the nucleon 4-momenta, the q_i are the pion 4-momenta, $u(p)$ is the usual Dirac wave function of the nucleon, and the invariant scalar functions $A(s,t)$ and $B(s,t)$ of the Mandelstam invariants $s = (p_1 + q_1)^2$, $t = (q_2 - q_1)^2$ realize the analytic properties of the S-matrix themselves in the complex s and t planes. This means that whenever we have spinning particles, we may focus on the analogs of A and B in Eq. (1) in isolating the respective analytic properties of the corresponding S-matrix elements. We note that Stuart [18] has emphasized this point in connection with the production and decay of Z pairs in e^+e^- annihilation and in connection with the production and decay of single W's in e^+e^- annihilation. What this means is that, in formulating the Laurent expansion of the S matrix about its poles to

isolate the dominant leading-pole term (the LPA is then realized by dropping all but this leading term), we may focus on only A and B, or we may insist that in evaluating the residues of the poles in the S-matrix the wave functions and kinematical covariants are also evaluated at the pole positions. When we focus only on the analogs of A and B in formulating the LPA, we shall refer to the result simply as the LPA_a; when we also evaluate the wave functions and kinematical covariants at the pole positions in isolating the poles in the analogs of A and B for the LPA, we shall refer to the respective result as the LPA_b. As Stuart stressed as well, both the LPA_a and the LPA_b are fully gauge invariant.

For the process under discussion, a general representation is [18]

$$\mathcal{M} = \sum_j \ell_j A_j(\{q_k q_l\}), \qquad (2)$$

where $\{\ell_j\}$ are a complete set of kinematical covariants which carry the same transformation properties as does $\mathcal{M}$, and the Lorentz scalars $\{q_k q_l\}$ are a complete set of Lorentz scalar invariants for the external 4-momenta of $\mathcal{M}$. In the LPA_a, we make a Laurent expansion of the A_j and retain

only their leading poles, without touching the $\{\ell_j\}$; in the LPA_b, we also evaluate the ℓ_j at the position of the respective leading poles. Evidently, in the latter case, we must make an analytic continuation of the phase-space point originally associated with the $\{\ell_j\}$ to a corresponding such point for the respective pole positions. See Ref. [12] for an illustration of such a continuation in the context of the YFS-exponentiated exact $\mathcal{O}(\alpha)$ calculation for the production process in $e^+e^- \rightarrow W^+W^- + n(\gamma) \rightarrow 4f + n(\gamma)$, and Refs. [5] for a similar illustration in the context of the $\mathcal{O}(\alpha)$ correction to $e^+e^- \rightarrow W^+W^- \rightarrow 4f$. Having isolated the appropriate realization of the LPA at the level of $\mathcal{M}$, it must still be decided whether to treat the phase space used to integrate the cross section exactly or approximately to match what was done for the $\{\ell_j\}$ in the case of the LPA_b. In all of our work, we stress that we always treat the exact phase space, both in the LPA_a and in the LPA_b.

In the context of YFS exponentiation, we realize the LPA as follows, as was briefly described already in Ref. [12]. Taking the respective 4-fermion plus n-photon process kinematics to be as given by (here, $d\tau_{n+4}$ is the respective phase space differential with the appropriate normalization):

$$e^-(p_1) + e^+(p_2) \rightarrow f_1(r_1) + \bar{f}_2(r_2) + f_1'(r_1') + \bar{f}_2'(r_2') + \gamma(k_1), \dots, \gamma(k_n)$$

$$\sigma_n = \frac{1}{\text{flux}} \int d\tau_{n+4}(p_1 + p_2; r_1, r_2, r_1', r_2', k_1, \dots, k_n)$$

$$\times \sum_{Ferm.\ spin} \sum_{Phot.\ spin} |\mathcal{M}_{4f}^{(n)}(p_1, p_2, r_1, r_2, r_1', r_2', k_1, \dots, k_n)|^2, \qquad (3)$$

and that of the corresponding W^+W^- production and decay process to be as given by

$$e^-(p_1) + e^+(p_2) \rightarrow W^-(q_1) + W^+(q_2),$$

$$W^-(q_1) \rightarrow f_1(r_1) + \bar{f}_2(r_2), \quad W^+(q_2) \rightarrow f_1'(r_1') + \bar{f}_2'(r_2'),$$

$$\sigma_n = \frac{1}{\text{flux}} \int d\tau_{n+4}(p_1 + p_2; r_1, r_2, r_1', r_2', k_1, \dots, k_n)$$

$$\times \sum_{Ferm.\ spin} \sum_{Phot.\ spin} |\mathcal{M}_{LPA}^{(n)}(p_1, p_2, r_1, r_2, r_1', r_2', k_1, \dots, k_n)|^2 \qquad (4)$$

in the context of YFS exponentiation [19,20], we proceed according to Refs. [12,19,20],

$$\mathcal{M}_{4f}^{(n)}(p_1, p_2, r_1, r_2, r_1', r_2', k_1, \dots, k_n)$$

$$\overset{LPA}{\rightarrow} \mathcal{M}_{LPA}^{(n)}(p_1, p_2, r_1, r_2, r_1', r_2', k_1, \dots, k_n)$$

$$= \sum_{Phot.\ partitions} \mathcal{M}_{Prod}^{(a),\lambda_1\lambda_2}(p_1, p_2, q_1, q_2, k_1, \dots, k_a)$$

$$\times \frac{1}{D(q_1)} \mathcal{M}_{Dec_1,\lambda_1}^{(b-a)}(q_1, r_1, r_2, k_{a+1}, \dots, k_b)$$

$$\times \frac{1}{D(q_2)} \mathcal{M}_{Dec_2,\lambda_2}^{(n-b)}(q_2, r_1', r_2', k_{b+1}, \dots, k_n),$$

$$D(q_i) = q_i^2 - M^2,$$

$$M^2 = (M_W^2 - i\Gamma_W M_W)[1 - \Gamma_W^2/M_W^2 + \mathcal{O}(\alpha^3)],$$

$$q_1 = r_1 + r_2 + k_{a+1} + \cdots + k_b,$$

$$q_2 = r_1' + r_2' + k_{b+1} + \cdots + k_n, \tag{5}$$

so that M^2 is the pole in the complex q^2 plane when q is the respective W 4-momentum, and M_W and Γ_W are the *on-shell* scheme mass and width, respectively. The residues in Eq. (5) are all defined at $q_i^2 = M^2$ with a prescription according to whether we have LPA_a or LPA_b, so that Eq. (5) is our YFS generalization of the formula in Eq. (12) in the first paper in Ref. [5]:

$$\mathcal{M}^{(n)} = \sum_{\lambda_1,\lambda_2} \Pi_{\lambda_1,\lambda_2}(M_1,M_2) \frac{\Delta_{\lambda_1}^+(M_1)}{D_1} \frac{\Delta_{\lambda_2}^-(M_2)}{D_2},$$

$$n = 0,1, \tag{6}$$

where $D_i = D(q_i)$ and $M_i^2 = M^2$. We stress that, unlike what is true of the formula in Eq. (12) in the first paper in Ref. [5] and in Eq. (6) here, in Eq. (5) n is arbitrary. The sum over "photon partitions" is over all 10^n possible attachments of n photons to the six external fermion lines and the two $W^\pm$ lines (one for the W production and one for the W decay, respectively). We make the further approximation that $M_i^2 = M_W^2$ in the residues in Eq. (5), always maintaining gauge invariance, as explained. Equations (3) and (4) in Ref. [21] then give us, in the presence of renormalization-group-improved perturbation theory, for the representation

$$\mathcal{M}_{LPA}^{(n)}(p_1,p_2,r_1,r_2,r_1',r_2',k_1,...,k_n)$$

$$= \sum_{j=0}^{\infty} \mathcal{M}_j^{(n)}(p_1,p_2,r_1,r_2,r_1',r_2',k_1,...,k_n), \tag{7}$$

where $\mathcal{M}_j^{(n)}$ is the jth virtual photon loop contribution to the residues in $\mathcal{M}_{LPA}^{(n)}$, the identifications

$$\mathcal{M}_j^{(n)}(p_1,p_2,r_1,r_2,r_1',r_2',k_1,...,k_n) = \sum_{r=0}^{j} \mathbf{m}_{j-r}^{(n)} \frac{(\alpha B')^r}{r!}, \tag{8}$$

where B' is now, for the LPA_b case to be definite, the *on shell* virtual YFS infrared function, which reduces to that given in Eqs. (8) and (9) in Ref. [20] when we restrict our attention to the production process, and α is indeed $\alpha(0)$ when it multiplies B' here. Let us keep this limit of B' in mind, as we focus on the gauge invariance of YFSWW3-1.11

in Ref. [12], which treats the radiation in the production process, and on that of YFSWW3-1.13 and YFSWW3-1.14, in which the radiation from the decay processes is also treated. In the LPA_a case, the corresponding B' function is *off shell*. Let us discuss first the LPA_b case and comment later on how the corresponding results for the LPA_a case are obtained.

Here, since the $SU(2)_L \times U(1)$ Ward-Takahashi identities require [see Eq. (47) in Ref. [22]]

$$k^\mu M_\mu^\gamma = 0, \quad k^\mu M_\mu^Z = i\sqrt{\mu_Z}M^x,$$

$$k^\mu M_\mu^{W^\pm} = \pm\sqrt{\mu_W}M^{\phi^\pm}, \tag{9}$$

for μ_V denoting the squared V boson mass (so that, for $V = W$, $\mu_W = M^2$), we find that B' is $SU(2)_L \times U(1)$ invariant from the equations in (9) and our result, Eq. (8), in Ref. [20]. From Eq. (8) it then follows that the infrared residuals $\mathbf{m}_{j-r}^{(n)}$ are also $SU(2)_L \times U(1)$ invariant. Here, χ and $\phi^\pm$ are the usual unphysical Higgs fields in our general renormalizable gauges and we use the notation of Ref. [22], so that M_μ^Z is their respective amplitude for the emission of a Z of Lorentz index μ and 4-momentum k, and M^x is their corresponding amplitude for the emission of a χ with the same 4-momentum, etc.

Introducing Eq. (8) into Eq. (7) gives

$$\mathcal{M}_{LPA_b}^{(n)}(p_1,p_2,r_1,r_2,r_1',r_2',k_1,...,k_n)$$

$$= e^{\alpha B'} \sum_{j=0}^{\infty} \mathbf{m}_j^{(n)}(p_1,p_2,r_1,r_2,r_1',r_2',k_1,...,k_n). \tag{10}$$

Equation (2.13) in Ref. [19] and Eq. (7) in Ref. [21] then give our n-photon differential cross section, for $P = p_1 + p_2$, $\vec{P} = 0$, as

$$d\sigma_{LPA_b}^n = e^{2\Re\alpha B'}\frac{1}{n!} \int \prod_{j=1}^{n} \frac{d^3k}{k_j^0} \delta^{(4)}\left(P - R - \sum_j k_j\right)$$

$$\times \left|\sum_{n'=0}^{\infty} \mathbf{m}_{n'}^{(n)}\right|^2 \frac{d^3r_1}{r_1^0}\frac{d^3r_2}{r_2^0}\frac{d^3r_1'}{r_1'^0}\frac{d^3r_2'}{r_2'^0}, \tag{11}$$

where we note that, when we only focus on the production process in Eq. (11), R is the produced WW intermediate state; $R = r_1 + r_2 + r_1' + r_2'$. Using the second theorem of the YFS program [Eq. (2.15) in [19]], we get

$$\left|\sum_{n'=0}^{\infty} \mathbf{m}_{n'}^{(n)}\right|^2 = \tilde{S}(k_1)\cdots\tilde{S}(k_n)\bar{\beta}_0 + \sum_{i=1}^{n} \tilde{S}(k_1)\cdots\tilde{S}(k_{i-1})\tilde{S}(k_{i+1})\cdots\tilde{S}(k_n)\bar{\beta}_1(k_i) + \cdots$$

$$+ \sum_{i=1}^{n} \tilde{S}(k_i)\bar{\beta}_{n-1}(k_1,\cdots,k_{i-1},k_{i+1},\cdots,k_n) + \bar{\beta}_n(k_1,\cdots,k_n), \tag{12}$$

where the real emission function $\tilde{S}(k)$ is given by $\tilde{S}_{Prod}(k)$, the real emission infrared function in Eq. (8) in Ref. [20] for *on shell* W's, when we only focus on the emission from the production process as we did in Refs. [12,13]. Since, in general,

$$\tilde{S}(k) = \tilde{S}_{Prod} + \tilde{S}_{Dec_1} + \tilde{S}_{Dec_2} + \tilde{S}_{Int}, \tag{13}$$

with

$$\tilde{S}_{Prod}(k) = -\frac{\alpha}{4\pi^2}\left[\left(\frac{p_1}{kp_1} - \frac{p_2}{kp_2}\right)^2 + \left(\frac{\mathcal{A}q_1}{k\mathcal{A}q_1} - \frac{\mathcal{A}q_2}{k\mathcal{A}q_2}\right)^2 + \left(\frac{p_1}{kp_1} - \frac{\mathcal{A}q_1}{k\mathcal{A}q_1}\right)^2 + \left(\frac{p_2}{kp_2} - \frac{\mathcal{A}q_2}{k\mathcal{A}q_2}\right)^2 - \left(\frac{p_1}{kp_1} - \frac{\mathcal{A}q_2}{k\mathcal{A}q_2}\right)^2 \right.$$
$$\left. -\left(\frac{p_2}{kp_2} - \frac{\mathcal{A}q_1}{k\mathcal{A}q_1}\right)^2\right]\Bigg|_{(\mathcal{A}q_i)^2 = M_W^2}, \tag{14}$$

$$\tilde{S}_{Dec_1}(k) = -\frac{\alpha}{4\pi^2}\left[Q_1 Q_2\left(\frac{r_1}{kr_1} - \frac{r_2}{kr_2}\right)^2 - Q_1 Q_W\left(\frac{r_1}{kr_1} - \frac{\mathcal{A}q_1}{k\mathcal{A}q_1}\right)^2 + Q_2 Q_W\left(\frac{r_2}{kr_2} - \frac{\mathcal{A}q_2}{k\mathcal{A}q_2}\right)^2\right]\Bigg|_{(\mathcal{A}q_1)^2 = M_W^2}, \tag{15}$$

$$\tilde{S}_{Dec_2}(k) = -\frac{\alpha}{4\pi^2}\left[Q_1' Q_2'\left(\frac{r_1'}{kr_1'} - \frac{r_2'}{kr_2'}\right)^2 + Q_1' Q_W\left(\frac{r_1'}{kr_1'} - \frac{\mathcal{A}q_2}{k\mathcal{A}q_2}\right)^2 - Q_2' Q_W\left(\frac{r_2'}{kr_2'} - \frac{\mathcal{A}q_2}{k\mathcal{A}q_2}\right)^2\right]\Bigg|_{(\mathcal{A}q_2)^2 = M_W^2}, \tag{16}$$

$$\tilde{S}_{Int}(k) = -\frac{\alpha}{4\pi^2}\left(\frac{p_1}{kp_1} - \frac{p_2}{kp_2} + Q_1\frac{r_1}{kr_1} - Q_2\frac{r_2}{kr_2} + Q_1'\frac{r_1'}{kr_1'} - Q_2'\frac{r_2'}{kr_2'}\right)^2 - \tilde{S}_{Prod} - \tilde{S}_{Dec_1} - \tilde{S}_{Dec_2} \tag{17}$$

is really composed of the scalar product of emission currents $\{j_b^\mu(k)\}$ with $k_\mu j_b^\mu(k) = 0$, Eq. (13) is also $SU(2)_L \times U(1)$ invariant. Here

$$\mathcal{A}q_i \equiv \text{analytical continuation of } q_i \text{ to the point } q_i^2$$
$$= M_W^2. \tag{18}$$

This analytical continuation, already described in Ref. [12], does not spoil the gauge invariance, as we see from Eqs. (13),(18). It follows that the hard-photon residuals $\{\bar{\beta}_n\}$ are also $SU(2)_L \times U(1)$ invariant.

Substitutung Eq. (12) into Eq. (11) we finally get the $SU(2)_L \times U(1)$-invariant expression, which is the fundamental formula of our calculation,

$$d\sigma_{LPA_b} = e^{2\Re\alpha B' + 2\alpha\tilde{B}}\frac{1}{(2\pi)^4}\int d^4 y \, e^{iy(p_1 + p_2 - q_1 - q_2) + D}$$
$$\times\left[\bar{\beta}_0 + \sum_{n=1}^{\infty}\frac{d^3 k_j}{k_j^0}e^{-iyk_j}\bar{\beta}_n(k_1, \ldots, k_n)\right]$$
$$\times\frac{d^3 r_1}{\bar{r}_1^0}\frac{d^3 r_2}{\bar{r}_2^0}\frac{d^3 r_1'}{\bar{r}_1'^0}\frac{d^3 r_2'}{\bar{r}_2'^0}, \tag{19}$$

where we have defined

$$D = \int\frac{d^3 k}{k_0}\tilde{S}[e^{-iy\cdot k} - \theta(K_{\max} - |\vec{k}|)],$$

$$2\alpha\tilde{B} = \int\frac{d^3 k}{k_0}\theta(K_{\max} - |\vec{k}|)\tilde{S}(k). \tag{20}$$

This shows that the parameter $K_{\max} \ll \sqrt{s}$ is a dummy parameter on which $d\sigma$ does not depend. In Eq. (19), when the complete value of $\tilde{S}(k)$ is used, then all $W^\pm$ radiative effects are contained in the respective $\bar{\beta}_n$ residuals, in accordance with the YFS theory in Ref. [19], as the non-zero widths of the W's prevent any IR singularities when a W radiates a photon in Eq. (4). In our work in YFSWW3, as we indicate below, we make the approximation of dropping all interference effects between the production and decay stages and between the two decay stages of Eq. (4). This means that we drop the $\tilde{S}_{Int}(k)$ in $\tilde{S}(k)$ in Eq. (13) and in Eq. (19), so that the YFS theory then determines the corresponding forms of the YFS functions $\bar{\beta}_n$, B' and D as also having the respective interferences dropped. This approximation, which resums a certain class of large W radiative effects, corresponds to the YFS exponentiation of the W production and decay radiation in the LPA, neglecting of all interferences between the production and decay stages and between the two decay processes.

All of the above results extend directly to the calculation when we use LPA_a amplitudes, as these are also gauge-invariant by the gauge invariance of our leading poles in the S matrix. Thus, the only change we must make is that the respective residues must be calculated in the LPA_a rather than in the LPA_b; for example, in Eqs. (14)–(17), q_i would be used instead of $\mathcal{A}q_i$, etc. We have done this, as we further illustrate in the following.

Let us now comment on the issue of the pure FSR YFS exponentiation for the decay processes treated in the LPA. We proceed in analogy to what is done in Ref. [23] for the MC YFS3 for the respective FSR. Specifically, for both decay residue amplitudes $\mathcal{M}_{Dec_i, \lambda_i}^{(n')}$, we may have contributions to the respective hard-photon residuals $\bar{\beta}_n$ due to emission for the final-state decay processes; in these we follow the procedure, described in Refs. [23,24], and already illustrated in

Ref. [25], for including these contributions, using the same YFS methods as we used above for radiative effects to the initial, intermediate, and final states. Here, we shall neglect all interference effects between the production and decay processes as we explained above; this is analogous to neglecting all interference effects between the initial and final states in the $\bar{\beta}_n$ in Refs. [23,25]. We note that it is possible to retain these interference effects, as we have illustrated in the exact $\mathcal{O}(\alpha)$ YFS-exponentiated BHWIDE MC in Ref. [26] for wide-angle Bhabha scattering and, more recently, using the new CEEX (coherent exclusive exponentiation) exponentiation theory in Ref. [27], to all orders in α in the new KK MC [24,27] for the two fermion processes from the τ threshold to 1 TeV. In this way we see that the use of Eq. (19) to include exponentiation of the FSR is fully realizable by the Monte Carlo methods we already tested. We stress that, for the same reasons we gave for the exponentiation of the complete process, these FSR contributions to the $\bar{\beta}_n$ are fully gauge invariant.

In the current version of YFSWW3, version 1.14, we also drop the $\tilde{S}_{Dec_i}$ terms in $\tilde{S}$ in Eq. (13) and the corresponding terms in the functions $\bar{\beta}_n$, B' and D, and include FSR using the program PHOTOS [28], which gives us a LL $\mathcal{O}(\alpha^2)$ realization of the FSR in which finite p_T effects are represented as they are in the $\mathcal{O}(\alpha)$ soft-photon limit. This LL implementation of FSR is fully gauge invariant. The ratios of the branching ratios (BRs) are then used to obtain the $\mathcal{O}(\alpha)$ correction in the normalization associated with the $\mathcal{O}(\alpha)$ correction to the decay processes themselves. Evidently, these ratios of BRs are also gauge invariant. As we illustrate below, for the corresponding non-factorizable corrections we use an efficient approximation in terms of the so-called screened Coulomb ansatz [29], which has been shown to be in good agreement with the exact calculations for singly inclusive distributions [29]. This ansatz is gauge invariant.

We also point out that the current version 1.14 differs from version 1.13 in Ref. [13] in that it uses a different renormalization scheme. Specifically, the scheme used in version 1.13 is the so-called G_μ of Ref. [30], in which the weak-scale coupling [30] α_{G_F} is used for all terms in the virtual correction, except those that are infrared singular, which are given the coupling $\alpha \equiv \alpha(0)$. In the renormalization-group-improved YFS theory, as formulated in Ref. [21], all the terms in the amplitude that involve corrections, in which the emitted photon of 4-momentum k has $k^2 \to 0$, should have the coupling strength corresponding to $\alpha(0)$—not just those that are IR singular. We therefore have introduced into YFSWW3 this requirement of the renormalization-group-improved YFS theory to arrive at version 1.14. We refer to this scheme as our scheme (A). According to the renormalization-group-improved YFS theory, it gives a better representation of the higher orders effects than does the G_μ scheme of Ref. [30]. We stress that this scheme (A) is also gauge invariant. The main effect of this change in renormalization scheme between versions 1.13 and 1.14 is to change the normalization of version 1.14 by $\sim$ -0.3% to -0.4% with respect to that of version 1.13 [11].

The generic size of the resulting shift in the YFSWW3 prediction which we just quoted can be understood by isolating the well-known soft plus virtual LL inital state radiation (ISR) correction to the process at hand, that has in $\mathcal{O}(\alpha)$ the expression [30]

$$\delta_{ISR,LL}^{v+s} = \beta \ln k_0 + \frac{\alpha}{\pi}\left(\frac{3}{2}L + \frac{\pi^2}{3} - 2\right),\qquad (21)$$

where $\beta \equiv (2\alpha/\pi)(L-1)$, $L = \ln(s/m_e^2)$, and k_0 is a dummy soft cut-off that cancels out of the cross section as usual. In the G_μ scheme of Refs. [30], which is used in YFSWW3-1.13, only the part $\beta \ln k_0 + (\alpha/\pi)(\pi^2/3)$ of $\delta_{ISR,LL}^{v+s}$ has the coupling $\alpha(0)$ and the remaining part of $\delta_{ISR,LL}^{v+s}$ has the coupling $\alpha_{G_\mu} \cong \alpha(0)/(1 - 0.0371)$. The renormalization-group-improved YFS theory implies, however, that $\alpha(0)$ should be used for all the terms in $\delta_{ISR,LL}^{v+s}$. This is done in YFSWW3-1.14 and results in the normalization shift $[(\alpha(0) - \alpha_{G_\mu})/\pi](1.5L - 2)$, which is $\sim -0.33\%$ at 200 GeV. This explains most of the change in the normalization of YFSWW3-1.14 with respect to YFSWW3-1.13. Moreover, it does not contradict the expected total precision tag of either version of YFSWW3 at their respective stages of testing. We stress that, according to the renormalization-group equation, version 1.14 is an improvement over version 1.13 in that it better represents the true effect of the respective higher-order corrections.

For the purposes of cross-checking with ourselves and with Ref. [16], we also created a second scheme, scheme (B), for the realization of the renormalization in YFSWW3-1.14. In this scheme, we put the entire $\mathcal{O}(\alpha)$ correction from Refs. [30] at the coupling strength $\alpha = \alpha(0)$. Since the pure NL hard $\mathcal{O}(\alpha)$ correction is only ~ -0.006 at 200 GeV, scheme (B) differs in the normalization from scheme A by $\sim [\alpha(0)/\alpha_{G_\mu} - 1] (-0.006) \cong 0.0002$, which is well below the 0.5% precision tag regime of interest for LEP2. Thus, scheme B, which is used in Ref. [16], is a perfectly acceptable scheme for LEP2 applications. It gives us a useful reference point from which to interpret our comparison with the results of RACOONWW from Ref. [16], which we discuss below.

Having presented our gauge-invariant calculation as it is realized in the MC YFSWW3-1.14, we will now turn to illustrating it in the context of LEP2 applications. Specifically, we always have in mind that one will combine the cross section from YFSWW3 with that from the KORALW-1.42 [14,15] MC, which is capable of calculating the nonresonant background contribution in a gauge-invariant way. We can do this in two ways, which we will now briefly describe, and we refer the reader to Refs. [31] for a more detailed discussion. In the first way, we start with LPA$_a$ and we denote the corresponding cross section from YFSWW3-1.14 as $\sigma(Y_a)$. It is corrected for the missing background contribution by adding to it a correction $\Delta\sigma(K)$ from KORALW-1.42 to form

$$\sigma_{Y/K} = \sigma(Y_a) + \Delta\sigma(K),\qquad (22)$$

where $\Delta\sigma(K)$ is defined by

$$\Delta\sigma(K) = \sigma(K_1) - \sigma(K_3).\qquad (23)$$

TABLE I. The total WW cross sections $\sigma_{WW} = \sigma(K_3)$, $\sigma(Y_4)$ at the Born and ISR level, the $4f$ corrections $\delta_{4f} = \Delta\sigma(K)/\sigma_{Born}(Y)$ and the $\mathcal{O}(\alpha)$ NL correction $\delta_{WW}^{NL} = \Delta\sigma(Y_a)/\sigma_{Born}(Y)$ at $E_{c.m.} = 200$ GeV. The numbers in parentheses are the statistical errors corresponding to the last digits of the results. All of the results are without cuts.

No cuts		σ^{WW} (fb)		δ_{4f} (%)		
Final state	Program	Born	ISR	Born	ISR	δ_{WW}^{NL} (%)
	YFSWW3	219.793 (16)	204.198 (09)	—	—	-1.92 (4)
$\nu_\mu \mu^+ \tau^- \bar{\nu}_\tau$	KORALW	219.766 (26)	204.178 (21)	0.041	0.044	—
	(Y$-$K)/Y	0.01 (1)%	0.01 (1)%	—	—	—
	YFSWW3	659.69 (5)	635.81 (3)	—	—	-1.99 (4)
$u\bar{d}\mu^- \bar{\nu}_\mu$	KORALW	659.59 (8)	635.69 (7)	0.073	0.073	—
	(Y$-$K)/Y	0.02 (1)%	0.02 (1)%	—	—	—
	YFSWW3	1978.37 (14)	1978.00 (09)	—	—	-2.06 (4)
$u\bar{d}s\bar{c}$	KORALW	1977.89 (25)	1977.64 (21)	0.060	0.061	—
	(Y$-$K)/Y	0.02 (1)%	0.02 (1)%	—	—	—

Here, the cross section $\sigma(K_1)$ is the complete 4-fermion result from KORALW-1.42 with all background diagrams and with the YFS-exponentiated $\mathcal{O}(\alpha^3)$ LL ISR and the cross section $\sigma(K_3)$ is the restricted CC03 Born-level result from KORALW-1.42—again with the YFS-exponentiated $\mathcal{O}(\alpha^3)$ LL ISR. The result in Eq. (22) is then accurate to $\mathcal{O}[(\alpha/\pi)(\Gamma_W/M_W)]$. Alternatively, one may start with the cross section for LPA$_{a,b}$ in YFSWW3-1.14, which we refer to as $\sigma(Y_a)$ and $\sigma(Y_b)$ correspondingly, and isolate the respective YFS-exponentiated $\mathcal{O}(\alpha)$ correction, $\Delta\sigma(Y)$, which is missing from the cross section $\sigma(K_1)$ as

$$\Delta\sigma(Y_j) = \sigma(Y_j) - \sigma(Y_4), \qquad (24)$$

where $\sigma(Y_4)$ is the corresponding cross section from YFSWW3-1.14, with the non-leading (NL) non-ISR $\mathcal{O}(\alpha)$ corrections to $\bar{\beta}_n$, $n = 0,1$, switched off. Then the cross section

$$\sigma_{K/Y} = \sigma(K_1) + \Delta\sigma(Y_j) \qquad (25)$$

has the accuracy of $\mathcal{O}[(\alpha/\pi)(\Gamma_W/M_W)]$. We have checked that the results $\sigma_{Y/K}$ and $\sigma_{K/Y}$ are numerically equivalent at the 0.1% level of interest to us here. In the following we only show results from the former. For completeness, we also note that we sometimes identify $\sigma(Y_1) = \sigma(Y_a)$, $\sigma(Y_2) = \sigma(Y_b)$, $\sigma(Y_3) = \sigma(K_3)$, and $\sigma(K_2)$ is to be identified as the cross section from KORALW-1.42 with the restricted on-pole CC03 Born-level matrix element with YFS-exponentiated $\mathcal{O}(\alpha^3)$ LL ISR. This latter cross section is a future option of KORALW [10]. It would allow further combinations of YFSWW3 and KORALW with the desired $\mathcal{O}[(\alpha/\pi)(\Gamma_W/M_W)]$ accuracy. Such combinations would be of use in cross-checks of our work.

We now illustrate our precision predictions using $\sigma_{Y/K}$. We have checked that the correction $\Delta\sigma(K)$ is small, $\lesssim 0.1\%$ for c.m.s. energies ~ 200 GeV. This is summarized in Tables I and II, in which we compare the size of the correction $\Delta\sigma(K)$, labeled δ_{4f}, with the size of the respective NL non-ISR $\mathcal{O}(\alpha)$ correction for the 4-lepton, 2-lepton–2-quark, and

TABLE II. The total WW cross sections $\sigma_{WW} = \sigma(K_3)$, $\sigma(Y_4)$ at the Born and ISR level, the $4f$ corrections $\delta_{4f} = \Delta\sigma(K)/\sigma_{Born}(Y)$ and the $\mathcal{O}(\alpha)$ NL correction $\delta_{WW}^{NL} = \Delta\sigma(Y_a)/\sigma_{Born}(Y)$ at $E_{c.m.} = 200$ GeV. The numbers in parentheses are the statistical errors corresponding to the last digits of the results. All of the results are with the *bare* cuts of Sec. 4.1 of Ref. [11].

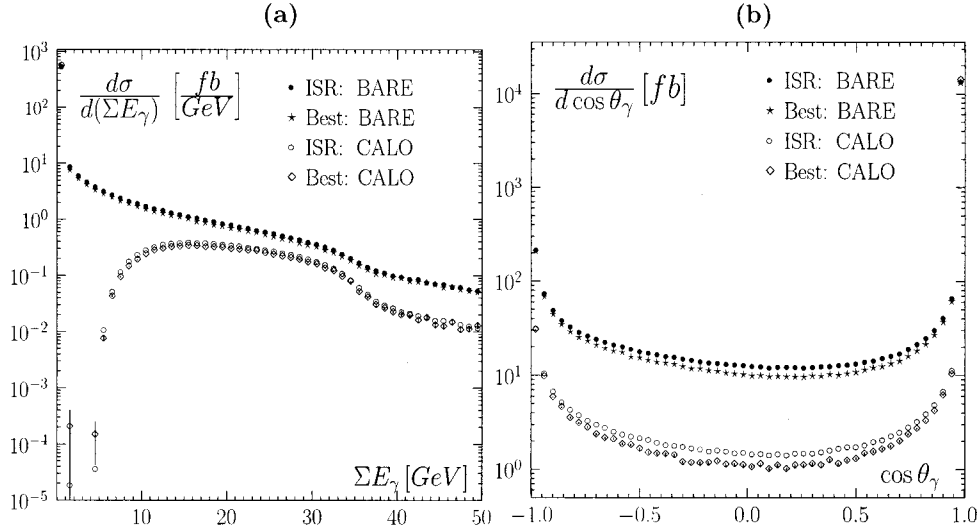| With cuts		σ^{WW} (fb)		δ_{4f} (%)		
Final state	Program	Born	ISR	Born	ISR	δ_{WW}^{NL} (%)
	YFSWW3	210.938 (16)	196.205 (09)	—	—	-1.93 (4)
$\nu_\mu \mu^+ \tau^- \bar{\nu}_\tau$	KORALW	210.911 (26)	196.174 (21)	0.041	0.044	—
	(Y$-$K)/Y	0.01 (1)%	0.02 (1)%	—	—	—
	YFSWW3	627.22 (5)	605.18 (3)	—	—	-2.00 (4)
$u\bar{d}\mu^- \bar{\nu}_\mu$	KORALW	627.13 (8)	605.03 (7)	0.074	0.074	—
	(Y$-$K)/Y	0.01 (1)%	0.02 (1)%	—	—	—
	YFSWW3	1863.60 (15)	1865.00 (09)	—	—	-2.06 (4)
$u\bar{d}s\bar{c}$	KORALW	1863.07 (25)	1864.62 (21)	0.065	0.064	—
	(Y$-$K)/Y	0.03 (2)%	0.02 (1)%	—	—	—

FIG. 1. Distributions of the total photon energy (a) and cosine of the hardest photon polar angle (b) for the $u\bar{d}+\mu\bar{\nu}_\mu+n(\gamma)$ final state. The solid, open circle, star, and diamond curves correspond to the LL BARE, LL CALO, $\mathcal{O}(\alpha)_{\mathrm{prod}}\,\mathcal{O}(\alpha^2)$ LL FSR BARE, and CALO YFS-exponentiated results, respectively.

4-quark final states, with and without the cuts of Ref. [11] at 200 GeV.

Thus, in what follows, we shall ignore $\Delta\sigma(K)$, as our ultimate precision tag objective, $<0.5\%$, does not require that we keep it. It will be analyzed in more detail elsewhere [10]. Further, for the cross section $\sigma(Y_a)$ we have already presented, for version 1.13, in Figs. 1–8 of Ref. [13], for the $c\bar{s}\ell^-\bar{\nu}_l$, $\ell=e^-$, μ^- final states, the $W^{+,-}$ angular distributions in the e^+e^- c.m.s. system, the $W^{+,-}$ mass distributions, the distributions of the final-state lepton energies in the laboratory frame (e^+e^- c.m.s. frame), and the final-state lepton angular distributions in the W^- rest frame and their corrections (relative to the Born level). The main effect on these differential distributions of the improved normalization of version 1.14 is to shift the normalization, as we discussed above. Thus, we do not repeat their presentation here. We refer the reader to the results in Ref. [13] for an investigation into the size of the EW=NL (EW denotes electroweak) and FSR effects in the cases listed above insofar as YFSWW3-1.14 is concerned with the understanding that the shapes of the distributions apply directly to version 1.14, but that the normalization of the EW correction should be reduced by -0.3% to -0.4%. In general, we found in Ref. [13] that, depending on the experimental cuts and acceptances, both the FSR and the EW corrections were important in precision studies of these distributions; this conclusion still holds for
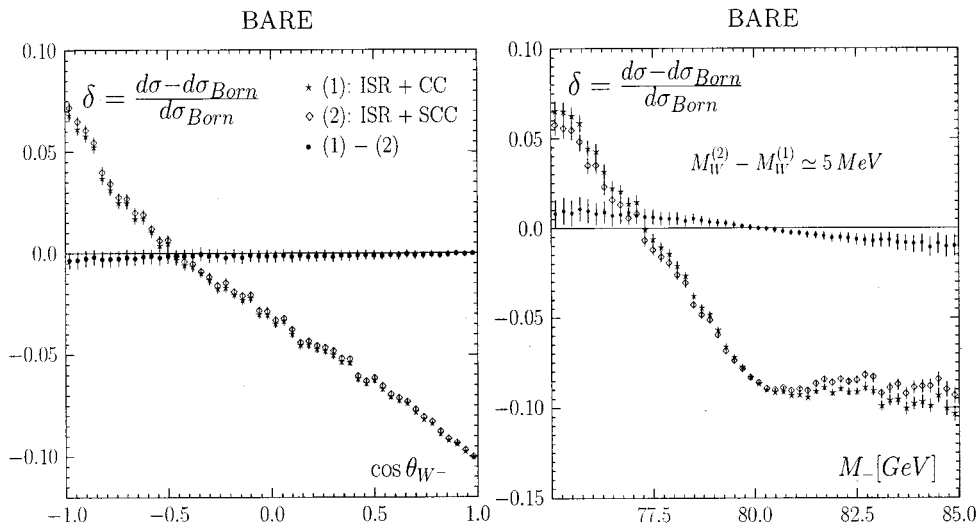

FIG. 2. Effects of the screened Coulomb correction (SCC) on the distributions of the polar angle (left) and the invariant mass (right) of W^- in comparison with the usual Coulomb correction (CC) at $E_{c.m.}=200$ GeV. As indicated the star, solid diamond, and large dotted curves are the ISR+usual Coulomb correction, ISR+screened Coulomb correction, and their difference respectively, in the presence of YFS exponentiation. Results are for the $e^+e^-\rightarrow W^+W^-\rightarrow u\bar{d}\mu^-\bar{\nu}_\mu$ channel. The *bare* cut is that of Sec. 4.1 of Ref. [11].

TABLE III. Total cross sections for CC03 from RACOONWW and YFSWW3 at $\sqrt{s}=200$ GeV without cuts. The numbers in parentheses are statistical errors corresponding to the last digits.

No cuts		σ_{tot} (fb)	
Final state	Program	Born	Best
	YFSWW3	219.770(23)	199.995(62)
$\nu_\mu \mu^+ \tau^- \bar{\nu}_\tau$	RACOONWW	219.836(40)	199.551(46)
	(Y−R)/Y	−0.03(2)%	0.22(4)%
	YFSWW3	659.64(07)	622.71(19)
$u\bar{d}\mu^- \bar{\nu}_\mu$	RACOONWW	659.51(12)	621.06(14)
	(Y−R)/Y	0.02(2)%	0.27(4)%
	YFSWW3	1978.18(21)	1937.40(61)
$u\bar{d}s\bar{c}$	RACOONWW	1978.53(36)	1932.20(44)
	(Y−R)/Y	−0.02(2)%	0.27(4)%

version 1.14, of course. For example, in the lepton decay angle distribution, for the BARE acceptance (BARE denotes that the final charged lepton is not combined with any photons) both the FSR and the EW correction modulate the distribution, whereas for the CALO acceptance of Ref. [13] (CALO denotes that all photons within 5° of the final-state charged lepton are combined with it) the FSR effect is almost nil whereas the EW correction effect remains at the level of $\sim$ 2.0%. Here, we focus on the total c.m.s. photon energy distribution [Fig. 1(a)], and the c.m.s. photon angular distribution [Fig. 1(b)]. We show these results both for the BARE and CALO acceptances, as defined in the 4-fermion section [11]. For definiteness and in the interest of being self-contained, we list the standard input parameter set that we use here and that is used in Ref. [11], as it is given in Eqs. (1)–(7) of the latter reference:

$$M_Z = 91.1867 \text{ GeV}, \quad 1/\alpha(0) = 137.0359895,$$

$$G_\mu = 1.16637 \times 10^{-5} \text{ GeV}^{-2}, \tag{26}$$

so that we use [11]

TABLE IV. Total cross sections for CC03 from YFSWW3 and RACOONWW at $\sqrt{s}=200$ GeV with the *bare* cuts of Sec. 4.1 in Ref. [11] (see the text). The numbers in parentheses are statistical errors corresponding to the last digits.

With *bare* cuts		σ_{tot} (fb)	
Final state	Program	Born	Best
	YFSWW3	210.918(23)	192.147(63)
$\nu_\mu \mu^+ \tau^- \bar{\nu}_\tau$	RACOONWW	211.034(39)	191.686(46)
	(Y−R)/Y	−0.05(2)%	0.24(4)%
	YFSWW3	627.18(07)	592.68(19)
$u\bar{d}\mu^- \bar{\nu}_\mu$	RACOONWW	627.22(12)	590.94(14)
	(Y−R)/Y	−0.01(2)%	0.29(4)%
	YFSWW3	1863.40(21)	1826.80(62)
$u\bar{d}s\bar{c}$	RACOONWW	1864.28(35)	1821.16(43)
	(Y−R)/Y	−0.05(2)%	0.31(4)%

$$1/\alpha(M_z) = 128.887,$$

$$\text{for} \quad M_Z = 91.1867 \text{ GeV}, \quad m_t = 175 \text{ GeV},$$

$$M_H = 150 \text{ GeV}, \quad \alpha_S(M_Z) = 0.119, \tag{27}$$

as well as

$$M_W = 80.350 \text{ GeV}, \quad \Gamma_Z = 2.49471,$$

$$\Gamma_W = 2.08699 \text{ GeV}. \tag{28}$$

Other input parameters such as light quark masses are also as given in Eqs. (1)–(7) of Ref. [11]. The masses M_W, M_Z are the respective physical on-shell renormalized masses. As in Ref. [11], in all of our numerical work, we use the approximation $M^2 = M_W^2 - i\Gamma_W M_W$ for the respective complex pole position.

In Fig. 1(a) we see that the total photon energy distributions are different for the BARE and CALO cases but that the NL non-ISR correction does not affect them strongly. In Fig. 1(b) we see that for both the BARE and CALO cases the NL correction does affect the photon angular distribution away from the beam directions, as we expect. Note that this is the NL correction implied by the YFS exponentiation of our exact $\mathcal{O}(\alpha)_{prod}$ correction. Finally, in Fig. 2 we show the effect in the W mass and angular distributions of using the screened Coulomb correction from Ref. [29], as against the usual Coulomb correction from Ref. [32]. The effect we see is a 5 MeV shift in the peak position, associated with the difference between the screened and usual Coulomb corrections; we see almost no effect, as expected, associated with this difference on the e^+e^- c.m.s. W angular distribution. Since we calculate the finite $p_T n(\gamma)$ corrections to these distributions, these results are new. Indeed, in Ref. [11] it is shown that the results from RACOONWW and YFSWW3 (Best) for the distribution in Fig. 1(a) differ by $\sim 20\%$ and, as we have the dominant $\mathcal{O}(\alpha^2)$ LL corrections to this distribution whereas in Fig. 20 in Ref. [11] the RACOONWW result only has the exact $\mathcal{O}(\alpha)$ Born result for the hard photon observable, we expect that most of this discrepancy would be removed if the dominant $\mathcal{O}(\alpha^2)$ LL corrections were included in the RACOONWW results. This has recently been confirmed in Ref. [33], where the authors of RACOONWW show that, when they include the latter corrections in their predictions for the $\cos \theta_\gamma$ distribution in Fig. 1(a), the discrepancy is reduced to the level of $\lesssim 5\%$. In summary, from the results in Ref. [13] and those presented here, we see that the FSR and EW corrections are necessary for a precision study of the distributions in the W-pair production and decay process at LEP2 energies.

We have made a detailed comparison between our results and those from Ref. [16] based on the program RACOONWW in the context of the LEP2 MC Workshop [11]. A complete unpublished preliminary description of the respective results of this comparison has appeared in Ref. [11]. Here, we focus on the normalization comparison of the two calculations at LEP2 energies. We show in Table III the comparison of the RACOONWW and YFSWW3-1.14 results for the cross sections

TABLE V. Total cross sections for CC03 from RACOONWW and YFSWW3 at $\sqrt{s} = 500$ GeV without cuts. The numbers in parentheses are statistical errors corresponding to the last digits.

No cuts		σ_{tot} (fb)	
Final state	Program	Born	Best
	YFSWW3	87.087(11)	89.607(32)
$\nu_\mu \mu^+ \tau^- \bar{\nu}_\tau$	RACOONWW	87.133(23)	90.018(27)
	(Y−R)/Y	−0.05(3)%	−0.46(5)%
	YFSWW3	261.377(34)	279.086(97)
$u\bar{d}\mu^- \bar{\nu}_\mu$	RACOONWW	261.400(70)	280.149(86)
	(Y−R)/Y	−0.01(3)%	−0.38(5)%
	YFSWW3	783.93(11)	868.14(31)
$u\bar{d}s\bar{c}$	RACOONWW	784.20(21)	871.66(27)
	(Y−R)/Y	−0.03(3)%	−0.41(5)%

as indicated, without cuts at 200 GeV (we have looked at the lower energies 184 and 189 GeV and the comparisons there are similar, if not better). In Table IV, we show the analogous comparisons with the LEP2 MC Workshop cuts as described in Ref. [11].

We see that for all channels considered, the two sets of results agree to the level of 0.3%. This gives a total precision estimate of 0.4% for the theoretical uncertainty on the 200 GeV c.m.s. energy WW signal cross-section normalization when allowance is made for further possible uncertainties in the higher-order radiative corrections and the implementation of the LPA [11]. This is a significant improvement over the originally quoted $\sim 2\%$ for this uncertainty when the NL non-ISR $\mathcal{O}(\alpha)$ corrections are not taken into account [34]. An effort to further reduce this 0.4% is in progress.

Finally, with an eye toward the LC projects, we have made simulations using YFSWW3-1.14 for a c.m.s. energy of 500 GeV. We show our results in Table V for the total cross section without cuts; here we again compare them to the corresponding ones from RACOONWW [16]. The NL corrections are significant in these results. Precision studies at LC

energies must take these effects into account. As expected, the percentage difference between YFSWW3-1.14 and RACOONWW remains below 0.5% at 500 GeV c.m.s. energy and is somewhat larger than at 200 GeV c.m.s. energy.

In summary, we have presented two recipes for combining YFSWW3 and KORALW-1.42 to arrive at a gauge-invariant calculation of the WW-pair production and decay in which the YFS-exponentiated exact $\mathcal{O}(\alpha)_{prod}$ corrections are taken into account as well as the $\mathcal{O}(\alpha^2)$ LL FSR and YFS-exponentiated $\mathcal{O}(\alpha^3)$ LL ISR corrections to the background processes. We have illustrated our calculation with several sample MC results and we have compared our results on the cross-section normalization with those on Ref. [11] at 200 GeV. In this way, a new precision tag of 0.4% has been established for this normalization, which represents a considerable improvement over the original result [34] of $\sim 2\%$ when NL non-ISR corrections are not taken into account.

ACKNOWLEDGMENTS

[1] G. 't Hooft and M. Veltman, Nucl. Phys. **B44**, 189 (1972); **B50**, 318 (1972); G. 't Hooft, *ibid.* **B35**, 167 (1971); M. Veltman, *ibid.* **B7**, 637 (1968).

[2] S. L. Glashow, Nucl. Phys. **22**, 579 (1961); S. Weinberg, Phys. Rev. Lett. **19**, 1264 (1967); A. Salam, in *Elementary Particle Theory: Relativistic Groups and Anodyticity (Nobel Symposium No. 8)*, edited by N. Svartholm (Almqvist and Wiksell, Stockholm, 1968), p. 367.

[3] W. Beenakker *et al.*, *WW Cross-Sections and Distributions in Physics at LEP2*, edited by G. Altarelli, T. Sjöstrand, and F. Zwirner (CERN, Geneva, 1996), Vol. 1, p. 79.

[4] W. Beenakker, F. A. Berends, and A. P. Chapovsky, Phys. Lett. B **435**, 233 (1998).

[5] W. Beenakker, F. A. Berends, and A. P. Chapovsky, Nucl. Phys. **B548**, 3 (1999); in *Proceedings of RADCOR 1998*, edited by J. Sola (World Scientific, Singapore, 1999), p. 528.

[6] D. L. Burke, in *Beyond the Standard Model 4*, edited by J. F. Gunion *et al.* (World Scientific, Singapore, 1995), p. 125.

[7] *Japan Linear Collider (JLC), Proceedings of the 5th Workshop*, edited by Y. Kurihara (KEK, Tsukuba, 1995).

[8] M. Piccolo, in *Frascati 1998, Bruno Touschek and the Birth of e^+e^- Physics*, edited by G. Isidori (INFN, Frascati, 1999), p. 131.

[9] P. M. Zerwas, in *Proceedings of the 1999 International Workshop on High-Energy Physics and Quantum Field Theory*, edited by B. B. Levchenko and V. I. Savrin (Moscow State University, Moscow, 2000), p. 152.

[10] S. Jadach *et al.* (unpublished).

[11] *Proceedings of the LEP2 MC Workshop*, edited by S. Jadach, G. Passarino, and F. Pittau (CERN, Geneva, 2000), pp. 1–135, 269–378, Report CERN 2000-009.

[12] S. Jadach, W. Płaczek, M. Skrzypek, B. F. L. Ward, and Z. Wąs, Phys. Lett. B **417**, 326 (1998).

[13] S. Jadach, W. Płaczek, M. Skrzypek, B. F. L. Ward, and Z. Wąs, Phys. Rev. D **61**, 113010 (2000).

[14] S. Jadach, W. Płaczek, M. Skrzypek, B. F. L. Ward, and Z. Wąs, Comput. Phys. Commun. **119**, 272 (1999); **94**, 216 (1996).

[15] M. Skrzypek *et al.*, Phys. Lett. B **372**, 289 (1996).

[16] A. Denner, S. Dittmaier, M. Roth, and D. Wackeroth, Phys. Lett. B **475**, 127 (2000); J. Phys. G **26**, 593 (2000); Eur. Phys. J. C **4**, 1 (2000); Nucl. Phys. **B587**, 67 (2000); and (private communication).

[17] R. J. Eden, P. V. Landshoff, D. I. Olive, and J. C. Polkinghorne, *The Analytic S-Matrix* (Cambridge University Press, Cambridge, England, 1966).

[18] R. G. Stuart, Nucl. Phys. **B498**, 28 (1997); Eur. Phys. J. C **4**, 259 (1998); in *Proceedings of the Ringberg Workshop: The Higgs Puzzle—What Can We Learn From LEP2, LHC, NLC, And FMC?*, Kingberg, Germany, 1996, edited by B. Kniehl (World Scientific, Singapore, 1997), p. 47; in *Proceedings of the First Latin American Symposium on High-Energy Physics, Particles and Fields VII EMPC and I-SILAFAE—Dedicated To Memory Of Juan Jose Giambiagi*, edited by J. C. D'Oliva, M. Klein-Kreisler, and H. Mendez (AIP, Woodbury, NY, 1997), p. 199.

[19] D. R. Yennie, S. Frautschi, and H. Suura, Ann. Phys. (N.Y.) **13**, 379 (1961).

[20] S. Jadach, W. Płaczek, M. Skrzypek, and B. F. L. Ward, Phys. Rev. D **54**, 5434 (1996).

[21] B. F. L. Ward, Phys. Rev. D **36**, 939 (1987); **42**, 3249 (1990).

[22] W. Beenakker *et al.*, Nucl. Phys. **B500**, 255 (1997).

[23] S. Jadach and B. F. L. Ward, Phys. Lett. B **274**, 470 (1992).

[24] S. Jadach, B. F. L. Ward, and Z. Wąs, Phys. Rev. D **63**, 113009 (2001).

[25] S. Jadach, B. F. L. Ward, and Z. Wąs, Comput. Phys. Commun. **79**, 503 (1994).

[26] S. Jadach, W. Płaczek, and B. F. L. Ward, Phys. Lett. B **390**, 298 (1997).

[27] S. Jadach, B. F. L. Ward, and Z. Wąs, Phys. Lett. B **449**, 97 (1999); Comput. Phys. Commun. **130**, 260 (1999).

[28] E. Barberio and Z. Wąs, Comput. Phys. Commun. **79**, 291 (1994) and references therein.

[29] A. P. Chapovsky and V. A. Khoze, Eur. Phys. J. C **9**, 449 (1999).

[30] J. Fleischer, F. Jegerlehner, and M. Zrałek, Z. Phys. C **42**, 409 (1989); K. Kołodziej and M. Zrałek, Phys. Rev. D **43**, 3619 (1991); J. Fleischer, K. Kołodziej, and F. Jegerlehner, *ibid.* **47**, 830 (1993); J. Fleischer *et al.*, Comput. Phys. Commun. **85**, 29 (1995) and references therein.

[31] S. Jadach, W. Płaczek, M. Skrzypek, B. F. L. Ward, and Z. Wąs, Comput. Phys. Commun. **140**, 432 (2001); **140**, 475 (2001).

[32] V. S. Fadin, V. A. Khoze, A. D. Martin, and W. J. Stirling, Phys. Lett. B **363**, 112 (1995); D. Bardin *et al.*, *ibid.* **317**, 213 (1993), and references therein.

[33] A. Denner, S. Dittmaier, M. Roth, and D. Wackeroth, Eur. Phys. J. C **20**, 201 (2001).

[34] D. G. Charlton, Int. J. Mod. Phys. A **15S1**, 352 (2000), and references therein.